Global J. Environ. Sci. Manage. 10(4): 1759-1774, Autumn 2024, Serial #40

Global Journal of Environmental Science and Management
(GJESM)

Homepage: https://www.gjesm.net/

Podcasts

ORIGINAL RESEARCH ARTICLE

Fine particulate matter concentration forecasting using long short-term memory network and meteorological inputs

T. Istiana[1,2], B. Kurniawan[1,*], S. Soekirno[1], A. Wihono[1], D.E. Nuryanto[2], B.A. Pertala[2], A. Sopaheluwakan[2,3]

[1] *Department of Physics, Universitas Indonesia, Depok, Indonesia*

[2] *Indonesia's Meteorological, Climatological, and Geophysical Agency, Central Jakarta, Jakarta, Indonesia*

[3] *World Meteorological Organization, Geneva, Switzerland*

ARTICLE INFO

Article History:
Received 01 March 2024
Revised 06 April 2024
Accepted 11 June 2024

Keywords:
Air pollution
Hybrid deep learning models
Long short term memory (LSTM)
Fine particulate matter ($PM_{2.5}$) forecasting

ABSTRACT

BACKGROUND AND OBJECTIVES: In metropolitan settings, the requirement to travel and participate in everyday tasks exposes numerous individuals to the harmful effects of air pollutants, specifically particulate matter 2.5, which has the potential to impact their well-being. Developing precise forecasting models is crucial in mitigating air pollution and providing accurate predictions for the people.
Nonetheless, the deficiency in acquiring observable data can frequently lead to unsatisfactory performance of forecasting models in various scenarios. The objective of this study is to address the issue by examining the most effective approaches for predicting the non-linear time-series data of daily particulate matter 2.5 concentration using meteorological inputs.
METHODS: The concentration data of particulate matter 2.5 at Central Jakarta and South Jakarta were collected using sensors from the United States of America Embassy in Indonesia and Indonesia's Meteorological, Climatological, and Geophysical Agency. Conversely, the meteorological information was collected through the Merra-2 satellite. This study introduces the long short-term memory deep learning model and contrasts it with the one-dimensional convolution neural network as well as their hybrid counterpart. The dataset is split into 80 percent training and 20 percent testing data. The root mean square and mean absolute error values are then calculated to determine the performance of the models.
FINDINGS: A combination of long short-term memory and fully connected layers using dropouts and early stopping patience techniques has been successfully developed to model the non-linear time-series data of daily particulate matter 2.5 concentration. The model effectively captured the patterns present in the historical data, resulting in outcomes that exhibited similar patterns. The long short-term memory model demonstrates an overall root mean square error and mean absolute error values of 18.53 micrograms per cubic meter and 14.92 micrograms per cubic meter in Central Jakarta and 19.4 micrograms per cubic meter and 15.61 micrograms per cubic meter in South Jakarta, where the best seasonal data were found to be in the June-July-August and December-January-February seasons respectively.
CONCLUSION: The air pollution forecasting models, which were created using both seasonal and overall time-series data, have the ability to predict air pollution levels by utilizing historical pollution data and meteorological inputs. The proposed long short-term memory model outperforms the one-dimensional convolution network and their hybrid combination. It has effectively surpassed the constraint of collecting observable data, attaining minimal error values on both sensors and satellite data, signifying a noteworthy progression compared to previous studies. Therefore, it might benefit areas lacking sufficient data, providing a valuable tool for air pollution mitigation.

DOI: 10.22034/gjesm.2024.04.16

This is an open access article under the CC BY license (http://creativecommons.org/licenses/by/4.0/).

NUMBER OF REFERENCES	NUMBER OF FIGURES	NUMBER OF TABLES
41	9	5

*Corresponding Author:
Email: *budhy.kurniawan@sci.ui.ac.id*
Phone: +62 821 2320 0619
ORCID: 0000-0002-9203-7438

Note: Discussion period for this manuscript open until January 1, 2025 on GJESM website at the "Show Article".

INTRODUCTION

In recent years, air pollution has become a major environmental problem that has attracted the attention of many people worldwide (Zhang *et al.*, 2021). In Jakarta, the air quality analysis shows that particulate matter heavily pollutes the city, with average air quality index (AQI) values of 20.71 micrograms per cubic meter $\mu g/m^3$ in 2019 (Santoso *et al.*, 2020). Fine particulate matter (PM2.5) is characterized by particles with an aerodynamic diameter less than 2.5 millimeters (mm), leading to increased mortality rates upon inhalation (Raaschou-Nielsen *et al.*, 2023). It is widely accepted that local biomass burning activities are the main source of air pollutants, such as PM2.5 (Jaiswal *et al.*, 2018). Anthropogenic emissions are also believed to be the key influences on $PM_{2.5}$ concentrations, where the meteorological conditions strongly affect the variations of $PM_{2.5}$ in the long term (Dahari *et al.*, 2020). $PM_{2.5}$ levels are influenced by numerous factors. Zhang *et al.* (2015) elucidated the correlation between meteorological conditions and the formation of air pollutants, emphasizing their influence on the levels of critical air pollutants. These levels exhibit variations across different across seasons and geological conditions. Meteorological parameters, such as temperature, wind speed and direction, humidity, precipitation, radiation, atmospheric pressure, and planetary boundary layer, have also been shown to influence $PM_{2.5}$ concentrations (Chen *et al.*, 2020). It should be emphasized that PM2.5 and meteorological data possess non-linear and dynamic attributes, rendering their accurate prediction challenging. With the growing utilization of big data and artificial intelligence, the implementation of deep learning has witnessed a surge in diverse domains. Deep learning possesses the capability to recognize patterns in the complexity of non-linear data, setting it apart from traditional models (Yang *et al.*, 2021). Through the implementation of deep learning, achieving more accurate $PM_{2.5}$ concentration forecasting in urban areas became feasible, making it an intriguing alternative in studying air quality (Xayasouk *et al.*, 2020). A study conducted by Huang and Kuo (2020) provided an example of the utilization of Long short-term memory (LSTM) and other deep learning models in air quality forecasting. The time-series features can be extracted since the current pollutants are influenced by the concentrations in the past and meteorological factors (Qin *et al.*, 2019). According to Kaimian *et al.* (2019), the LSTM model could accurately explain 80 percent (%) of the observed $PM_{2.5}$ concentration variability by capturing the time series' temporal dependencies, improving the forecasting accuracy. Hence, the utilization of the LSTM model could potentially be employed for the purpose of forecasting the levels of various air pollutants (Kaimian *et al.*, 2019). The time-series prediction accuracies using the LSTM model are generally higher than other deep neural networks since the model can recall past experiences (Kim *et al.*, 2019). It is more stable in long-term series cases (Kim *et al.*, 2018). The rate of error growth tends to be slower in comparison to the recurrent neural network (RNN) model as the prediction time extends. The LSTM modeling technique has proven its capability to predict air quality time-series data (Krishan *et al.*, 2019). Qin *et al.*, (2019) highlighted how combining LSTM and convolution neural network (CNN) models can effectively tackle spatiotemporal challenges, achieving a more feasible application of deep learning for air pollution forecasting. The PM2.5 forecasting methodology in this study can be perceived as a fusion of three primary phases: data pre-processing, analysis of time-series data (utilizing pre-processed historical data), and data modeling. The models were developed using three deep learning models: LSTM, one-dimensional convolution neural network (1DCNN), and hybrid 1DCNN-LSTM, and were analyzed using the root mean square error (RMSE) and the mean absolute error (MAE) metric values. The investigation of optimal models for forecasting non-linear time-series data of daily PM2.5 presents a solution to address numerous challenges. This study primarily focuses on collecting inputs from sensors situated in the vicinity, enabling a comprehensive analysis. However, it is important to acknowledge constraints of sensors' limitation in gathering observable data. This study aims to tackle the challenges by ntegrating both sensors and satellite data, developing a combination of LSTM and fully connected layers using dropouts and early stopping patience techniques as one of the $PM_{2.5}$ concentration forecasting alternatives. The study has been carried out in Central Jakarta and South Jakarta with inputs from 2015 to 2023.

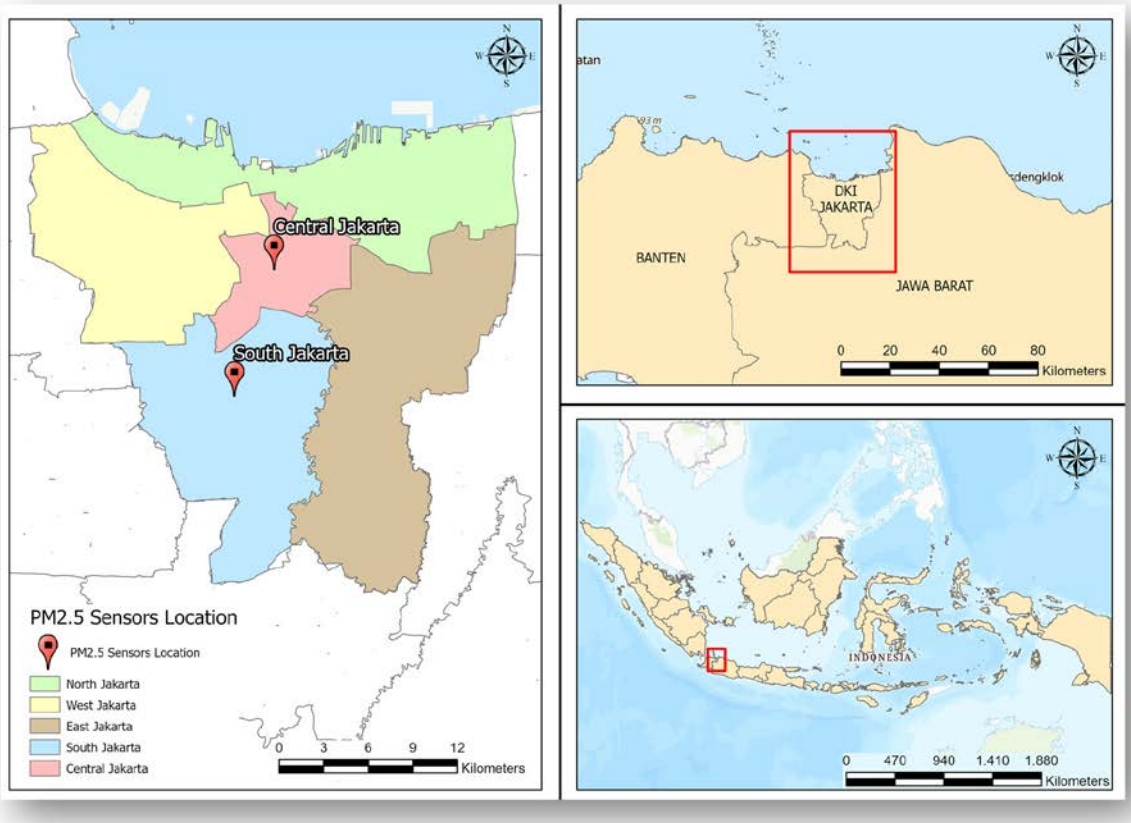


Fig. 1: Geographic location of the study area based on $PM_{2.5}$ sensors locations in the central and south Jakarta, Indonesia

MATERIALS AND METHODS

The present study provides a comprehensive explanation of various aspects, including the data gathering process, experimental environmental setup, study flowchart, models development, and evaluation parameters. Each of these components is elucidated in detail, ensuring a thorough understanding of the research methodology employed..

Data collection

The daily Air quality idex (AQI) data used in this study were obtained from the World Air Quality Index project. As shown in Fig. 1., this study was conducted in Central Jakarta (–6.18098, 106.83021) and South Jakarta (–6.25521, 106.80699). The $PM_{2.5}$ data were collected using sensors from the United States (US) Embassy in Indonesia and Indonesia's Meteorological, Climatological, and Geophysical Agency (BMKG). The data obtained from Central Jakarta spans from December 25, 2015, to September 18, 2023, whereas the data collected from South Jakarta covers the period from December 25, 2015, to May 22, 2023. Daily meteorological inputs were obtained from the Merra-2 satellite data by entering the latitude and longitude according to the sensors. The meteorological data obtained from the satellite is a reanalysis of global atmospheric data produced by the National Aeronautics and Space Administration (NASA). The meteorological parameters consist of the Temperature at 2 meters (T2M) degree Celsius (°C), Dew Point (DEW) (°C), Relative Humidity at 2 meters (RH2M) (%), Precipitation (PREC) millimeters per day (mm/day), Surface Pressure (PS) kilopascal (kPa), Wind Speed at 10 meters (WS10M) meter per second (m/s), and the Wind Direction at 10 meters (WD10M) (degree). It is imperative to comprehend that the environmental attributes of Central Jakarta and South Jakarta areas different. The sensors in Central

Jakarta are positioned in close proximity to the roadside, amidst a landscape dominated by business complexes, towering skyscrapers, and heavy traffic flow, which collectively account for the majority of emissions in the area. In contrast, the South Jakarta region is characterized by numerous residential areas (Istiana *et al.,* 2023).

Experimental environment setup

The anticipated LSTM model, which is a component of the RNN and deep learning, is projected to surmount the intricacy and vulnerability of non-linear data. The LSTM network is developed using Google Colab and Google Cloud with Keras deep learning library to create prediction models and solve time-series problems. Pandas and Sklearn libraries are also employed for data manipulation and analysis.

Study flowchart

As shown in Fig. 2., the study flowchart involves determining the datasets, developing models, forecasting data, and analyzing metric values.

In handling missing values, the mean-before-after method is used for the missing value imputation in the data pre-processing process. The mean-before-after method replaces the missing value on time l with the average value on time $i+1$ in the future and the value on time $i-1$ in the past, which can be described using Eq. 1 (Nath *et al.,* 2021).

$$\overline{x_l} = \frac{x_{i-1} + x_{i+1}}{2} \tag{1}$$

Nath *et al.* (2021) demonstrated the effectiveness of the mean-before-after method as a valuable imputation tool, particularly in the context of managing air pollutant data. Following the imputation process for missing values, the dataset was organized according to the seasonal variations in Indonesia, which are significantly impacted by monsoon activities. The seasonal data can then be categorized as the December-January-February (DJF) season, which represents the peak of the northwest Australian-Asian monsoon; June-July-August (JJA) season, which represents the peak of the Southeast Australian-Asian monsoon; and the March-April-May (MAM) and September-October-November (SON) seasons, which represent the monsoon transition (Istiana *et al.,* 2023). The process of data normalization involves utilizing the min-max normalization technique to scale the input values within a specified range of 0 to 1. This straightforward method allows for the manipulation of data within set boundaries. It can be described using Eq. 2 (Lima and Souza, 2023):

$$x = \frac{x - min}{max - min} \tag{2}$$

The initial step involves dividing the dataset into two parts: 80 percent for training and 20 percent for testing purposes. Subsequently, the Keras library's time-series generator is employed to convert the multivariate series data into a supervised learning model. This conversion process automatically transforms the time-series data, making it suitable for training. The parameters used in this model are as follows.

- Targets and features used in the model.
- The length of each sample used for the trained model, which in this case is 4.
- Sampling rate, a parameter represents the period between two output sub-series, which in this case is 1. Each output sub-series will be spaced one period apart.
- Batch size = 2, a parameter represents the number of output sub-series per batch. In this model, only two sub-series will be generated per batch.
- Shuffle = False, a parameter which tells the function not to randomize the sequence.

Model development

Deep learning was initially proposed by Dechter (1986). Later, Hochreiter and Schmidhuber (1997) introduced LSTM, a part of deep learning. LSTM is a type of RNN capable of exhibiting temporal dynamic behavior for time sequences (Greff *et al.,* 2017), learning long-term dependencies, and is not affected by exploding gradient problems (Sareen *et al.*, 2023). The structure of the LSTM model is shown in Fig. 3a. and Eqs. 3-8 (Sun *et al.,* 2021):

$$f_t = \sigma\left(W_f h_{t-1} + U_f x_t + b_f\right), \tag{3}$$

$$i_t = \sigma\left(W_i h_{t-1} + U_i x_t + b_i\right), \tag{4}$$

$$g_t = \tanh\left(W_g h_{t-1} + U_g x_t + b_g\right), \tag{5}$$

$$o_t = \sigma\left(W_o h_{t-1} + U_o x_t + b_o\right), \tag{6}$$

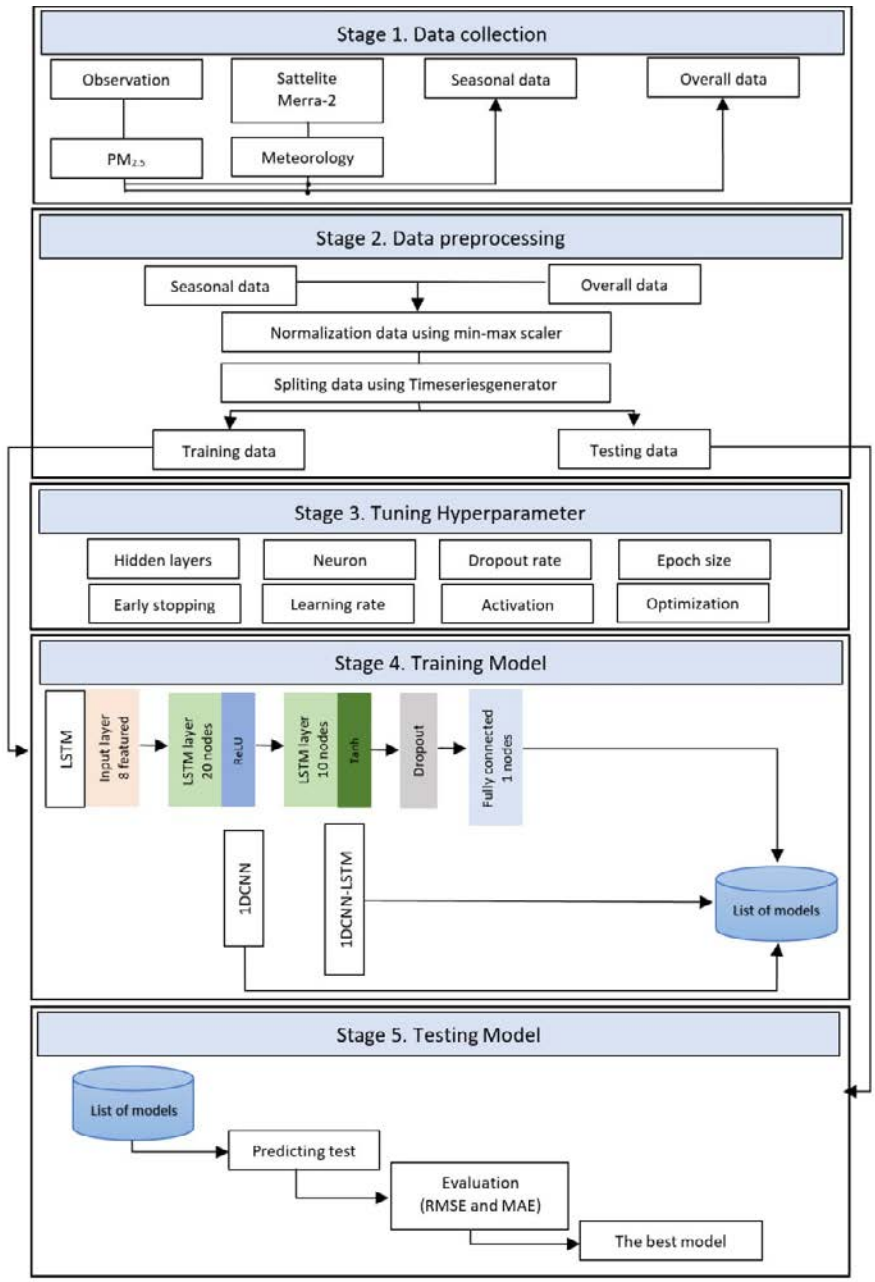


Fig. 2: The study flowchart

$$c_t = i_t \odot g_t + c_{t-1} \odot f_t, \quad (7)$$

$$h_t = tanh(c_t) \odot o_t. \quad (8)$$

Where;

t and $t-1$ are the time at the present and the previous time. The LSTM set consists of three gates and two nodes. Forget gate f_t, input gate i_t, output gate o_t, input node g_t, and cell state node $c_t.h_t$ are the results of one LSTM cell at a time t.

The input weights consist of W_f, W_i, W_g, and W_o,

while the output weights consist of U_f, U_i, U_g, and U_o. The bias, on the other hand, consists of b_f, b_i, b_g, and b_o. The sigmoid function is symbolized by σ, while the activation function and Hadamard's multiplication are indicated as tanh(.) and $\odot$, respectively (Sun *et al.,* 2021). The Hadamard operation is a binary operation with two matrices of the same dimension. The sigmoid function produces an output that falls within the range of 0 to 1, indicating the degree to which the input is transmitted through the structure. The forget gate, denoted as, f_t, determines the total cell states, c_{t-1}, that can currently be maintained; the input and output gates are used to save to input to the current cell, c_t, and to control the information output from the cell state (Zou *et al.,* 2023). The adjustment of the activation function, also referred to as the hyperparameter, is necessary in the LSTM model. Hyperparameters include the sigmoid function, hyperbolic tangent function (tanh), rectified linear unit (ReLU), dropout, and optimization adaptive moment estimation (Adam). serves as an activation function commonly employed in multiclass classification scenarios (Dubey *et al.,* 2022), while Optimization Adam is a first-order stochastic-based optimization technique utilized to reduce the loss function throughout the neural network training process (Chang *et al.,* 2019). The network structure of the convolution neural networks can generally be categorized into 1D-CNN, 2D-CNN, and 3D-CNN (Li *et al.*, 2020). The 3D-CNN is commonly used for image and video data identification (Vrskova *et al.*, 2022). In contrast, the 2D-CNN is typically employed for recognizing images and text (Mao *et al.*, 2022), while the 1D-CNN is frequently employed in the processing of time-series data (Abdeljaber *et al.,* 2017). This study utilized the 1D-CNN model as it is well-suited for processing time-series data. The process from 1DCNN can be illustrated through Fig. 3b, with the time-series input as a multidimensional matrix convoluting from top to bottom (Li *et al.*, 2020). The

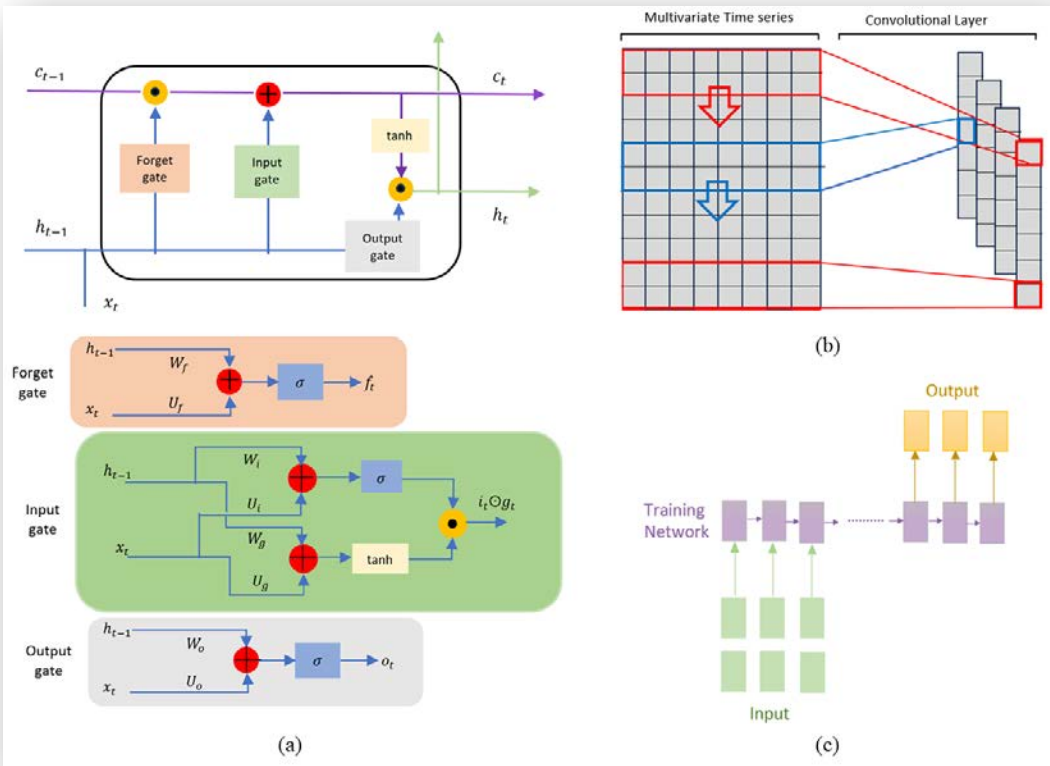


Fig. 3: (a) The structure of the LSTM model; (b) The process of 1D CNN; and (c) A simple network of the hybrid CNN-LSTM model

red color indicates the filter. The number of feature dimensions extracted after convolution with filters is represented by N^*1, whereas N represents the input dimension, filter size, and convolution step length. Blue represents a distinct filtering mechanism, which is then followed by additional filters. Let's assume that the total number of filters is denoted as M, and the resulting feature dimensions are represented by N^* M. The convolution layer serves as a feature to learn about the local trends. Each subsequent layer examines the non-linear depiction of the preceding layer. After the convolution layer was processed, a flattened layer was employed to transform the high-level representation into a feature vector. Subsequently, connected layers were utilized to decrease the dimensions of the ultimate output vector (Du *et al.,* 2016). The hybrid CNN-LSTM model is then built by combining CNN with LSTM. CNN is adopted for feature extraction, while LSTM is used to study past time-series data characteristics to predict air pollution concentrations (Qi *et al.,* 2019). Fig. 3c, represents a simple network of the hybrid CNN-LSTM. The input is represented by a light green color, the proposed CNN-LSTM hybrid model is symbolized by purple, and the output is indicated by yellow (Li *et al.*, 2020).

Model evaluation parameters

Two statistical metrics are employed to assess the precision and effectiveness of the models: MAE and RMSE. Generally, a lower error value signifies a superior performance of the prediction model. The calculations of MAE and RMSE are defined using Eqs. 9-10 (Sun *et al.,* 2021), with y_i as the actual $PM_{2.5}$ concentration, $\hat{y}_i$ as the predicted $PM_{2.5}$ concentration, $\overline{y}_i$ as the mean of the observed values, and n as the expected length of the test set.

$$MAE = \frac{1}{n}\sum_{i=1}^{n}|y_i - \hat{y}_i|, \quad (9)$$

$$RMSE = \sqrt{\frac{1}{n}\sum_{i=1}^{n}(y_i - \hat{y}_i)^2} \quad (10)$$

RESULTS AND DISCUSSION

The $PM_{2.5}$ forecasting models are evaluated. The models were developed following data pre-processing stage. The temporal variation of $PM_{2.5}$ concentration aimed to gain insights into its dispersion patterns throughout various seasons. Given the significant impact of meteorological parameters on $PM_{2.5}$ concentration, the correlations between them were also analyzed to determine which parameters should be incorporated into the developed models.

Temporal variation of $PM_{2.5}$ concentration

As shown in Fig. 4, the lowest concentrations of $PM_{2.5}$ in Central Jakarta and South Jakarta were observed in 2017 due to the La Nina phenomenon (Istiana *et al.,* 2023). The highest $PM_{2.5}$ concentration in Central Jakarta in 2016 was 105.55 $\mu g/m^3$, while the highest in the South Jakarta location in 2019 was 125.77 $\mu g/m^3$. The June-July-August season witnessed the highest average peak of PM2.5 concentrations in Central Jakarta and South Jakarta. In July, the Central Jakarta area reached its highest level at 115.64 µg/m^3, whereas the South Jakarta region recorded a peak of 126.95 µg/m^3 during the same period. This finding affirms that the occurrence of low temperatures and wind speeds during the dry season (JJA season), when the Asian-Australian northwest monsoon reaches its peak, results in the entrapment of air pollutants and the creation of particles (Istiana *et al.,* 2023). Another study by Jaiswal *et al.* (2018) similarly supports that the concentration of particulate matters typically peaks during the dry season. On the contrary, during the December-January-February period, there was a decrease in PM2.5 levels. In Central Jakarta, the least concentration was recorded in January at 70.61 µg/m^3, whereas South Jakarta experienced its lowest level in December at 77.75 µg/m^3. This indicates that the rainy season contributes to purifying the air by reducing PM2.5 levels (Istiana *et al.,* 2023).

Correlation between meteorological parameters and $PM_{2.5}$

The Pearson correlation results (r) described the correlation between $PM_{2.5}$ concentrations and meteorological parameters using time-series and seasonal data in both locations (Fig. 5. and Table 1). Correlation analysis is subsequently performed to gain a deeper understanding of the variations in PM2.5 concentrations and the impact of meteorological factors. Based on the Pearson correlation heatmap, there is a positive correlation between PM2.5 concentrations and temperature as well as pressure at both locations. In Central Jakarta, $PM_{2.5}$ concentration shows a strong negative correlation

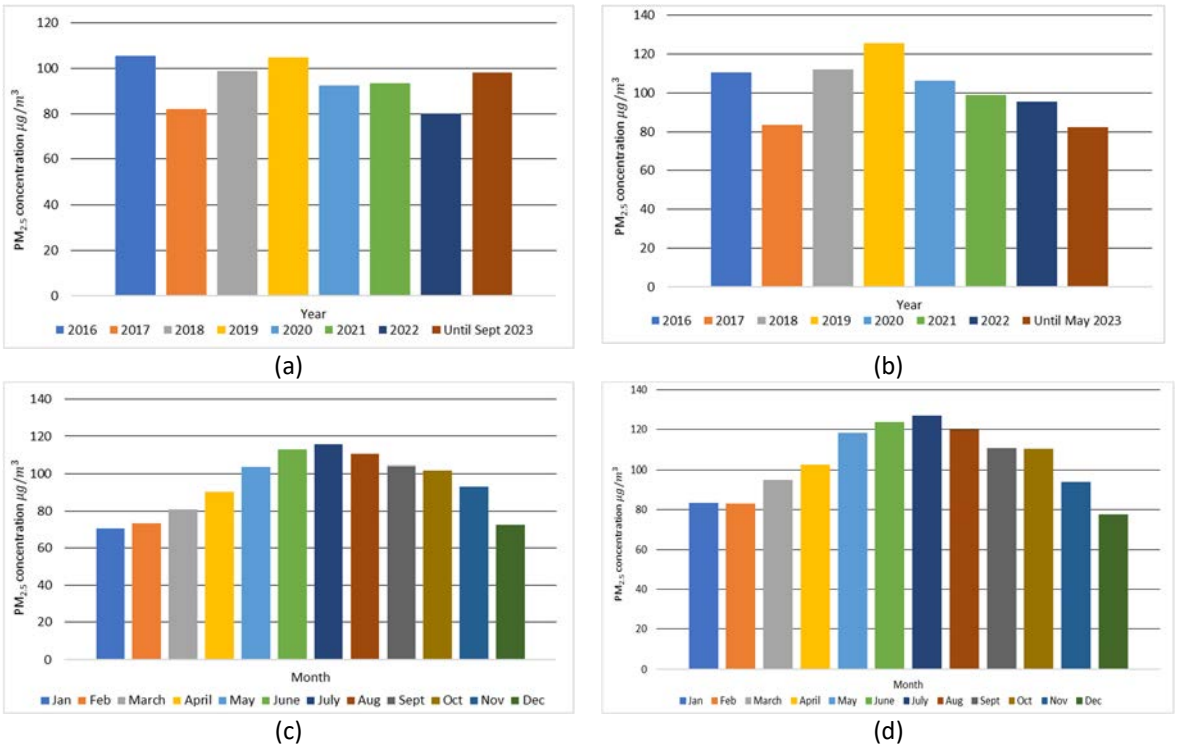


Fig. 4: (a) Annual temporal variation of $PM_{2.5}$ concentrations in Central Jakarta; (b) Annual temporal variation of $PM_{2.5}$ concentrations in South Jakarta; (c) Monthly temporal variation of $PM_{2.5}$ concentrations in Central Jakarta; and (d) Monthly temporal variation of $PM_{2.5}$ concentrations in South Jakarta

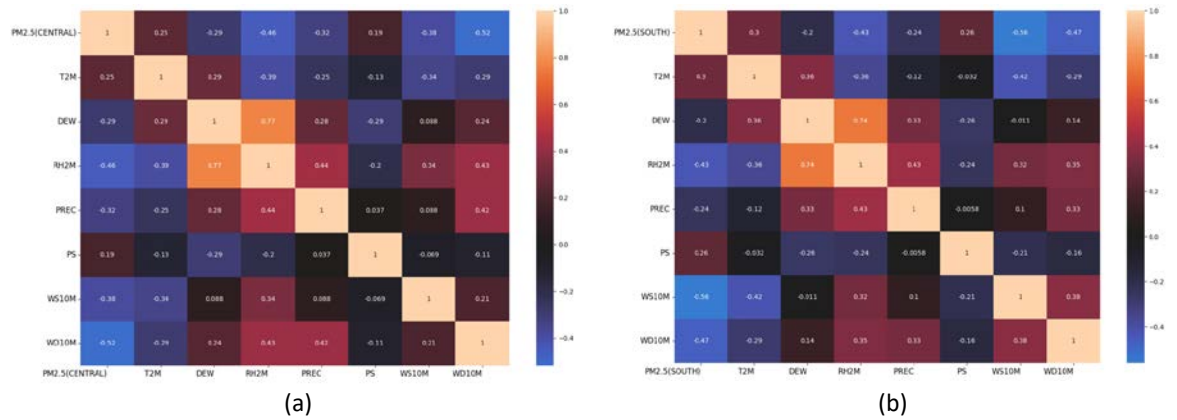


Fig. 5: (a) Pearson correlation using overall data in Central Jakarta; and (b) Pearson correlation using overall data in South Jakarta

with WD10M and RH2M with values of -0.52 and -0.46. On the other hand, $PM_{2.5}$ concentration shows a negative correlation with WS10M and WD10M in South Jakarta, with a value of -0.56 and -0.47.

The analysis has been conducted on seasonal variations to determine the correlations within the time-series data spanning from 2015 to 2023. In Fig. 5. and Table 1, the correlation between $PM_{2.5}$ and meteorological parameters varied with the seasons. $PM_{2.5}$ is positively correlated with temperature

Table 1: Pearson correlation using seasonal data in Central Jakarta and South Jakarta

Location	Meteorological Parameters						
	T2M	DEW	RH2M	PREC	PS	WS10M	WD10M
Seasonal Data (Central Jakarta)							
DJF	0.42	-0.008	-0.39	-0.13	0.08	-0.62	-0.27
MAM	0.45	-0.02	-0.4	-0.24	0.07	-0.28	-0.41
JJA	0.02	-0.16	-0.23	-0.21	0.18	-0.08	-0.07
SON	0.21	-0.32	-0.39	-0.23	0.21	-0.3	-0.34
Seasonal Data (South Jakarta)							
DJF	0.56	0.3	-0.4	-0.02	0.2	-0.61	-0.29
MAM	0.5	0.15	-0.34	-0.1	0.08	-0.47	-0.38
JJA	-0.06	-0.25	-0.31	-0.24	0.14	-0.31	0.02
SON	0.39	-0.33	-0.47	-0.21	0.32	-0.38	-0.35

Table 2: The settings of hyperparameters

Parameter	Value
Training set	80%
Testing set	20%
Win_length	4
Batch_size	2
Loss	MSE
Optimizer	Adam
Epochs	50
Learning rate	0.0005
Patience of early stopping mechanism	20

(T2M) in all seasons in Central Jakarta and almost in all seasons in South Jakarta. Similarly, In Central Jakarta, PM2.5 concentrations are minimally affected by pressure across all seasons, while in South Jakarta, pressure has a moderate impact on PM2.5 concentrations specifically during the SON season.

The LSTM network proposed

Deep learning models can be constructed by utilizing the meteorological parameters that exhibit substantial impacts, after conducting an in-depth analysis of the associations between PM2.5 concentrations and these parameters. It is essential for all the inputs, including meteorological data, to be pre-processed using the min-max normalization function. The data needs to be transformed into supervised learning data through the time-series generator prior to being fed into the models. The LSTM, 1DCNN, and hybrid 1DCNN-LSTM networks are then developed using $PM_{2.5}$ concentration and meteorological inputs to forecast $PM_{2.5}$ concentrations, with Mean Square Error (MSE) acting as the loss function to measure the differences between observed and forecasted data. Table 2 displays the parameter configurations employed in the comprehensive proposed model.

The developed LSTM network consists of an input, LSTM-1, LSTM-2, dropout, and fully connected layers (Fig. 6). Referring to Table 3, the first comprises 20 nodes that employ ReLU activation and possess a return sequence (True). In comparison, the second layer consists of 10 nodes with tanh activation and a return sequence (False Following this, the third layer is responsible for implementing dropouts, while the fourth layer represents the fully connected layer employing linear activation. The ReLU activation function can solve non-linear problems (Varshney and Singh, 2021) since it can enhance the feature maps' non-linear capabilities (Shao and Kim, 2022). The ReLU function serves to mitigate the issue of gradient vanishing of the tanh function (Dubey *et al*., 2022).

Fig. 7a-b, illustrates the loss function of the LSTM model, describing the models' performance by evaluating the MSE relatives to the number of epochs. This approach aids in mitigating underfitting and overfitting issues while identifying the most suitable model. The reduction in errors with increasing epochs signifies enhancements achieved during the training

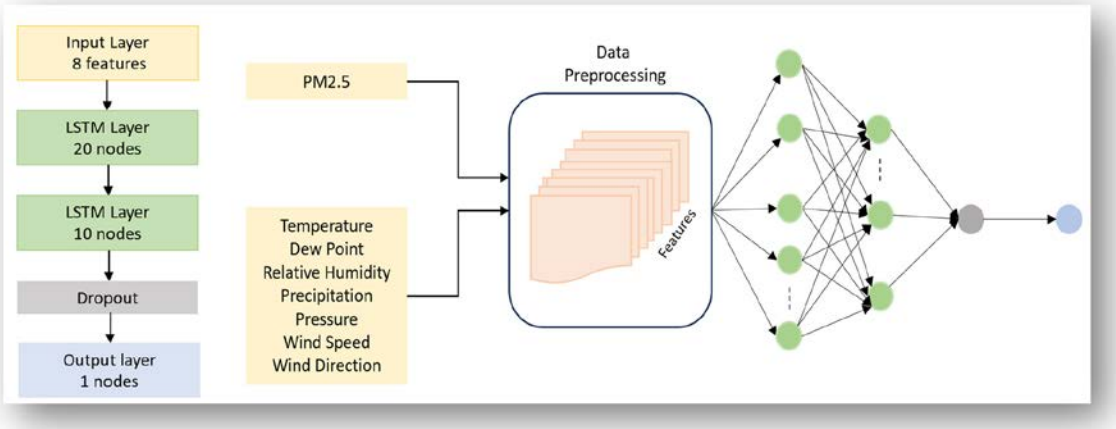


Fig. 6: The network system of the proposed LSTM neural network

Table 3: The proposed attribute LSTM neural network

Attribution	First layer	Second layer	Third Layer	Fourth layer
Layer type	LSTM	LSTM	Dropout	FC
Number of nodes	20	10	0	1
Number of parameters	2320	1240	0	11
Activation function	ReLU	Tanh		Linear
Remark	Return sequences true	Return sequences false	Rate 0.3. recurrent dropout (0.0)	
	Recurrent activation sigmoid			

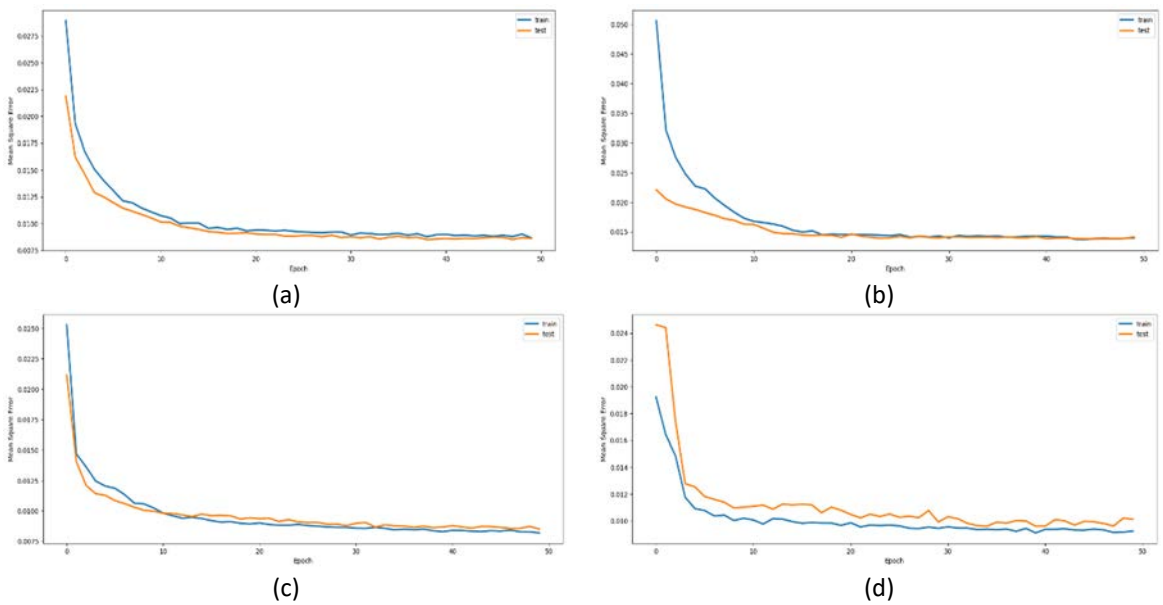


Fig 7: (a) Loss function of LSTM model in Central Jakarta; (b) Lost function of LSTM model in South Jakarta; (c) Loss function of LSTM model with a dropout rate of 0.1 in Central Jakarta; (d) Loss function of LSTM model with a learning rate of 0.005 in Central Jakarta

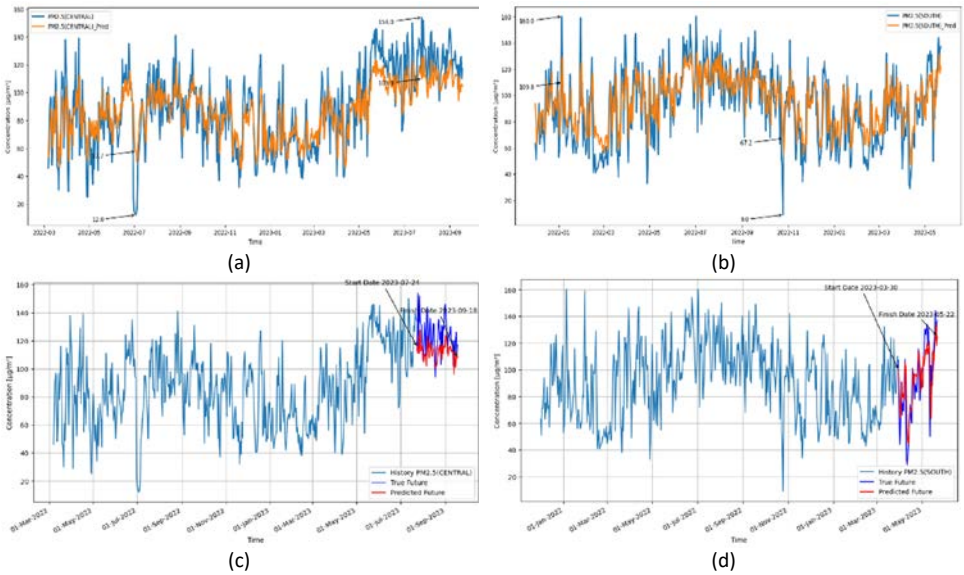


Fig. 8: (a) Comparison of $PM_{2.5}$ history and $PM_{2.5}$ prediction in Central Jakarta; (b) Comparison of $PM_{2.5}$ history and $PM_{2.5}$ prediction in South Jakarta; (c) Predicted future results in Central Jakarta and (d) Predicted future results in South Jakarta.

process. As epochs progress, the gradual decline in errors indicates a steady enhancement in the model's accuracy (Tabrizi *et al.,* 2021). Data overfitting can also be prevented using several techniques: regularization (Santos and Papa, 2022), data augmentation (Maharana *et al.*, 2022), dropouts (Xiao *et al.*, 2021), early stopping patience techniques (Gal and Ghahramani, 2016), and dropconnect (Hssayni *et al.*, 2022). Validation is typically performed in the early stopping patience methods during the training process and halted prior to reaching convergence in order to prevent overfitting (Gal and Ghahramani, 2016). During the initial phases of the model training procedure, it is hypothesized that the model will need numerous epochs in order to attain optimal outcomes. To achieve that goal, dropouts and early stopping patience technique are used in this study to prevent overfitting. Overfitting is a condition where the model performs well only during training, producing worse prediction results (Santos and Papa, 2022). The optimal dropout rate subsequently discovered to be 0.3 (Table 3). Referring to Fig. 7c, the decrease in dropout rate to 0.1 causes a slight overfitting. The testing loss curve is above the training loss curve, indicating higher error rates. Additionally, this study found revealed that a rise in the learning rate from 0.0005 to 0.005 resulted in notable overfitting and instability (Fig. 7d). Referring to Utku *et al.* (2023), it can then be concluded that the best combination and configuration of the models can only be achieved by tuning the hyperparameters. The study assessed the hyperparameters to determine the optimal settings, enhancing the proposed models and addressing any constraints.

The recognition of historical PM2.5 concentrations data trends was successfully achieved by the LSTM model, which stands as a significant highlight in this research (Fig. 8). Moreover, the model successfully predicted $PM_{2.5}$ trends in both locations over almost two months (Figs. 8c-d), yielding similar patterns, not the exact values. In South Jakarta, the lowest concentration was predicted to be 67.2 $\mu g/m^3$, while the actual value was 9.0 $\mu g/m^3$. The highest concentration had an expected value of 67.2 $\mu g/m^3$, while the actual value was 109.8 $\mu g/m^3$. On the other hand, in Central Jakarta, the lowest concentration was predicted to be 57.71 $\mu g/m^3$, while the actual value was 12.0 $\mu g/m^3$. Meanwhile, the highest concentration had a predicted value of 109.93 $\mu g/m^3$, while the actual value was 154 $\mu g/m^3$.

The evaluation of the models' performance can be done by interpreting the RMSE and MAE results of both the seasonal and overall time-series data, as shown in Fig. 9. The diagrams illustrate the lowest

RMSE and MAE values of the overall time-series data: 18.53 and 14.92 $\mu g/m^3$ in Central Jakarta; 19.40 and 15.61 $\mu g/m^3$ in South Jakarta. They also provide the lowest RMSE and MAE results for seasonal data: 16.64 and 13.64 $\mu g/m^3$ in Central Jakarta (JJA season); 19.31 and 15.45 $\mu g/m^3$ in South Jakarta (DJF season). Among all the developed models, LSTM achieved the best performance with the lowest error values. However, consistent with previous studies, LSTM required the longest training time, followed by the 1DCNN-LSTM and 1DCNN models (Li *et al.*, 2020).

Tables 4 and 5 illustrate the correlation

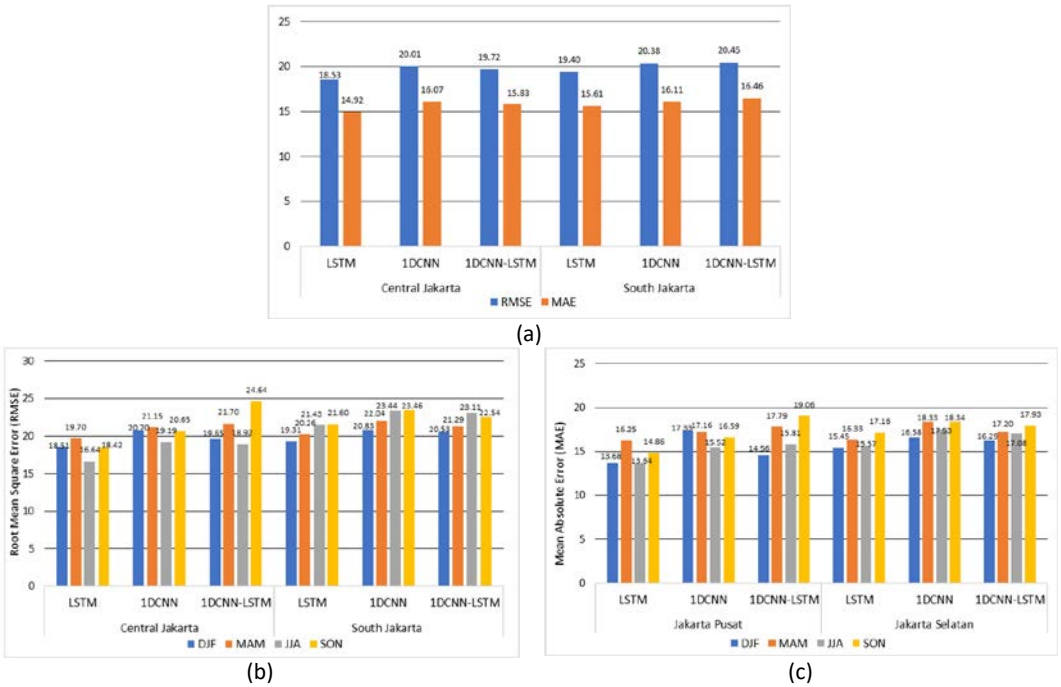


Fig. 9: (a) RMSE and MAE results comparison of each model for the overall time-series data; (b) RMSE results comparison for the seasonal data; (c) MAE results comparison for the seasonal data

Table 4: The correlation results of historical and predicted $PM_{2.5}$ overall time-series data

Location	Data history	$PM_{2.5}$ prediction		
		LSTM	1DCNN	1DCNN-LSTM
Central Jakarta	$PM_{2.5}$	0.78	0.71	0.78
South Jakarta		0.71	0.67	0.71

Table 5: The correlation results of historical and predicted $PM_{2.5}$ seasonal data

Location	Seasonal	Data History	$PM_{2.5}$ prediction		
			LSTM	1DCNN	1DCNN-LSTM
Central Jakarta	DJF	$PM_{2.5}$	0.61	0.52	0.55
	MAM		0,69	0.65	0.64
	JJA		0.60	0.61	0.61
	SON		0.71	0.63	0.73
South Jakarta	DJF		0.6	0.59	0.59
	MAM		0.62	0.58	0.56
	JJA		0.30	0.36	0.31
	SON		0.63	0.60	0.60

results between the predicted and actual $PM_{2.5}$ concentrations. The correlation results range between 0.67 and 0.78 for the overall time-series data, while they range from 0.30 to 0.71 for the seasonal data. During the SON season in Central Jakarta, all the deep learning models exhibited their optimal performance, whereas they demonstrated subpar performance during the JJA season in South Jakarta.

CONCLUSION

To summarize, the LSTM model has been effectively constructed using non-linear time-series data of daily $PM_{2.5}$ concentrations and meteorological inputs in Central Jakarta and South Jakarta. During the DJF season, the monsoon activities contribute to a decline in PM2.5 concentrations, as evidenced by the temporal variation observed in both locations. The correlation analysis described a strong correlation between $PM_{2.5}$ concentrations and meteorological parameters, such as RH2M, WS10M, and WD10M, which were then used as the main parameters. The proposed model integrates LSTM layers with dropouts and fully connected layers and incorporates early stopping patience strategies. The LSTM model achieved better forecasting results than the 1DCNN and 1DCNN-LSTM models, producing better RMSE and MAE results. Using overall time-series data, the best RMSE and MAE values were: 18.53 and 14.92 $\grave{\imath}\,g/m^3$ in Central Jakarta; 19.40 and 15.61 $\mu g/m^3$ in South Jakarta. Deep learning models have also been utilized for seasonal analysis to examine the impact of monsoon activities on the prediction of PM2.5 levels. The best RMSE and MAE in Central Jakarta were found during the June-July-August season with 16.64 and 13.64 $\mu g/m^3$. In contrast, the best RMSE and MAE in South Jakarta were found during the December-January-February season with 19.31 and 15.45 $\mu g/m^3$. The calculations of the mean square error were then used to describe the loss function of the LSTM models. The gradual decrease in errors over time signifies the successful convergence and prevention of overfitting by the proposed models as epochs progress steadily. The historical and forecasted $PM_{2.5}$ correlation results were also found ranging from 0.71 to 0.78 in Central Jakarta and from 0.67 to 0.71 in South Jakarta, with the best results occurring during the SON season. These findings point to the fact that every model possesses formidable skills in detecting patterns within historical data and utilizing them for predictive. The historical data were found to be related to future data to some extent, providing the necessary information for the forecasting models. The models have aptly reproduced the patterns found in historical data, generating consistent trend outcomes. Significantly, the model has effectively tackled the constraint of collecting observable data, leading to low error values on sensors and satellite data. Furthermore, utilizing the air quality parameters, tuning the hyperparameters, and adding more inputs has the potential to enhance the models' performance even more, providing valuable insights for future studies on air pollution forecasting.

AUTHOR CONTRIBUTIONS

T. Istiana performed the literature review, experimental design, analyzed and interpreted the data, and prepared the manuscript text and edition. B. Kurniawan performed literature review, manuscript text preparation, and manuscript edition. S. Soekirno performed the literature review and prepared the manuscript text. A. Wihono performed literature review, manuscript text preparation, and manuscript edition. D.E. Nuryanto analyzed the data and interpreted the data. B.A. Pertala performed the experimental design. A. Sopaheluwakan analyzed and interpreted the data.

ACKNOWLEDGEMENT

The authors would like to express their sincere gratitude to the Ministry of Research, Technology, and Higher Education of the Republic of Indonesia for the grant of Hibah Penelitian Disertasi Doktor [No: NKB-1130/UN2.RST/HKP.05.00/2023] provided to Mr. Budhy Kurniawan, the Education and Training Center of Indonesia's Meteorological, Climatological, and Geophysical Agency, and the National Research and Innovation Agency of Indonesia. The authors are grateful to the individuals who assisted by providing data from the US Embassy in Indonesia and Indonesia's Meteorological, Climatological, and Geophysical Agency.

CONFLICT OF INTEREST

The authors declare that there is no conflict of interests regarding the publication of this manuscript. In addition, the ethical issues, including plagiarism, informed consent, misconduct, data fabrication and/or falsification, double publication and/or submission, and redundancy have been completely observed by

the authors.

OPEN ACCESS

©2024 The author(s). This article is licensed under a Creative Commons Attribution 4.0 International License, which permits use, sharing, adaptation, distribution and reproduction in any medium or format, as long as you give appropriate credit to the original author(s) and the source, provide a link to the Creative Commons license, and indicate if changes were made. The images or other third-party material in this article are included in the article's Creative Commons license, unless indicated otherwise in a credit line to the material. If material is not included in the article's Creative Commons license and your intended use is not permitted by statutory regulation or exceeds the permitted use, you will need to obtain permission directly from the copyright holder. To view a copy of this license, visit: http://creativecommons.org/licenses/by/4.0/.

PUBLISHER'S NOTE

GJESM Publisher remains neutral with regard to jurisdictional claims in published maps and institutional afflictions.

ABBREVIATIONS

%	Percent
1DCNN	1 – Dimension convolution neural network
1 D C N N - LSTM	1 – Dimension convolution neural network - long short-term memory
2DCNN	2 – Dimension convolution neural network
3DCNN	3 – Dimension convolution neural network
$\mu g / m^3$	Microgram per cubic meters
σ	Sigmoid function
AQI	Air quality index
b	Bias weight
BMKG	Badan Meteorologi Klimatologi dan Geofisika (Indonesia's Meteorological, Climatological and Geophysical Agency)
c_t	Cell state node
°C	Degrees Celsius
DEW	Dew point
DJF	December-January-February
f_t	Forget gate
g_t	Input node
h_t	The result of one LSTM cell at a time t
i_t	Input gate
JJA	June-July-August
kPA	Kilo pascal
$PM_{2.5}$	Particulate matter 2.5
LSTM	Long short-term memory
MAE	Mean absolute error
MAM	March-April-May
mm	Millimeters
mm/day	Millimeters per day
m/s	Meter per second
n	The predicted length of the test set
o_t	Output gate
PREC	Precipitation
PS	Pressure
ReLU	Rectified linear unit
RH2M	Relative humidity at 2 meters
RMSE	Root mean square error
RNN	Recurrent neural network
SON	September-October-November
T2M	Temperature at 2 meters
tanh(.)	Activation function
U	Output weight
US	United State
W	Input weight
WD10M	Wind direction at 10 meters
WS10M	Wind speed at 10 meters
$\overline{x_l}$	Result mean before after method
x_{i-1}	Average of the value in the future
x_{i+1}	Average of the value in the last
y_i	Actual value
$\hat{y}_i$	Prediction value
$\overline{y}_i$	The average of the observed values

REFERENCES

1. Abdeljaber, O.; Avci, O.; Kiranyaz, S.; Gabbouj, M.; Inman, D.J., (2017). Real-time vibration-based structural damage detection using one-dimensional convolutional neural networks. J. Sound Vib., 388: 154–170 **(17 pages).**
2. Chang, Z.; Zhang, Y.; Chen, W., (2019). Electricity price prediction based on hybrid model of Adam optimized LSTM neural network and wavelet transform. Energy. 187: 115804 **(12 pages).**
3. Chen, Z.; Chen, D.; Zhao, C.; Kwan, M.; Cai, J.; Zhuang, Y.; Zhao, B.; Wang, X.; Chen, B.; Yang, J.; Li, R.; He, B.; Gao, B.; Wang, K.; Xu, B., (2020). Influence of meteorological conditions on $PM_{2.5}$ concentrations across China: A review of methodology and mechanism. Environ. Int., 139: 105558 **(21 pages)**.
4. Dahari, N.; Latif, M.T.; Muda, K.; Hussein, N., (2020). Influence of meteorological variables on suburban atmospheric $PM_{2.5}$ in the southern region of peninsular Malaysia. Aerosol Air Qual. Res., 20(1): 14–25 **(12 pages)**.
5. Dechter, R., (1986). Learning while searching in constraint satisfaction problems. Proceedings of the AAAI Conference on Artificial Intelligence, 5: 178–183 **(6 pages)**.
6. Du, X.; Cai, T.; Wang, S.; Zang, L., (2016). Overview of deep Learning. Proceedings of the Youth Academic Annual Conference of Chinese Association of Automation (YAC). 159–164 **(6 pages)**.
7. Dubey, S.R.; Singh, S.K.; Chaudhuri, B.B., (2022). Activation functions in deep learning: a comprehensive survey and benchmark. Neurocomputing. 503: 92–108 **(17 pages)**.
8. Gal, Y.; Ghahramani, Z., (2016). A theoretically grounded application of dropout in recurrent neural networks. Advances in neural information processing systems. 29 (NIPS 2016): 1019–1027 **(9 pages)**.
9. Greff, K.; Srivastava, R.K.; Koutnik, J.; Steunebrink, B.R.; Schmidhuber, J., (2017). LSTM: a search space odyssey. IEEE Trans. Neural Networks Learn. Syst., 28(10): 2222–2232 **(11 pages)**.
10. Hochreiter, S.; Schmidhuber, J., (1997). LSTM 1997. Neural Comput., 9(8): 1735–1780 **(46 pages)**.
11. Hssayni, E.H.; Joudar, N.E.; Ettaouil, M., (2022). An adaptive drop method for deep neural networks regularization: estimation of dropconnect hyperparameter using generalization gap. Knowledge-Based Syst., 253: 109567 **(10 pages)**.
12. Huang, C.J.; Kuo, P.H., (2018). A deep CNN-LSTM model for particulate matter ($PM_{2.5}$) forecasting in smart cities. Sensors. 18(7): 2220 **(22 pages)**.
13. Istiana, T.; Kurniawan, B.; Soekirno, S.; Nahas, A.; Wihono, A.; Nuryanto, D.E.; Adi, S.P.; Hakim, M.L., (2023). Causality analysis of air quality and meteorological parameters for $PM_{2.5}$ characteristics determination: evidence from Jakarta. Aerosol Air Qual. Res., 23(9): 1–18 **(18 pages)**.
14. Jaiswal, A.; Samuel, C.; Kadabgaon, V.M., (2018). Statistical trend analysis and forecast modeling of air pollutants. Global J. Environ. Sci. Manage., 4(4): 427–438 **(12 pages)**.
15. Kaimian, H.; Li, Q.; Wu, C.; Qi, Y.; Mo, Y.; Chen, G.; Zhang, X.; Sachdeva, S., (2019). Evaluation of different machine learning approaches to forecasting $PM_{2.5}$ mass concentrations. Aerosol Air Qual. Res., 19(6): 1400–1410 **(11 pages)**.
16. Kim, H.S.; Park, I.; Song, C.H.; Lee, K.; Yun, J.W.; Kim, H.K.; Jeon, M.; Lee, J.; Han, K.M., (2019). Development of a daily PM_{10} and $PM_{2.5}$ prediction system using a deep long short-term memory neural network model. Atmos. Chem. Phys., 19(20): 12935–12951 **(17 pages)**.
17. Kim, K.; Kim, D.K.; Noh, J.; Kim, M., (2018). Stable forecasting of environmental time series via long short-term memory recurrent neural network. IEEE Access. 6: 75216–75228 **(13 pages)**.
18. Krishan, M.; Jha, S.; Das, J.; Singh, A.; Goyal, M.K.; Sekar, C., (2019). Air quality modelling using long short-term memory (LSTM) over NCT-Delhi, India. Air Qual, Atmos. Health. 12(8): 899–908 **(10 pages)**.
19. Li, T.; Hua, M.; Wu, X., (2020). A hybrid CNN-LSTM model for forecasting particulate matter ($PM_{2.5}$). IEEE Access, 8: 26933–26940 **(8 pages)**.
20. Lima, F.T.; Souza, V.M.A., (2023). A large comparison of normalization methods on time series. Big Data Res., 34: 100407 **(15 pages).**
21. Maharana, K.; Mondal, S.; Nemade, B., (2022). A review: data pre-processing and data augmentation techniques. Global Transitions Proceeding. 3(1): 91–99 **(9 pages)**.
22. Mao, Y.; Zhang, Y.; Jiao, L.; Zhang, H., (2022). Document-level sentiment analysis using attention-based bi-directional long short-term memory network and two-dimensional convolutional neural network. Electronics. 11(12): 1906 **(15 pages)**.
23. Nath, P.; Saha, P.; Middya, A.I.; Roy, S., (2021). Long-term time-series pollution forecast using statistical and deep learning methods. Neural Comput. Appl., 33: 12551–12570 **(20 pages)**.
24. Qi, Y.; Li, Q.; Karimian, H.; Liu, D., (2019). A hybrid model for spatiotemporal forecasting of $PM_{2.5}$ based on graph convolutional neural network and long short-term memory. Sci. Total Environ., 664: 1–10 **(10 pages)**.
25. Qin, D.; Yu, J.; Zou, G.; Yong, R.; Zhao, Q.; Zhang, B., (2019). A novel combined prediction scheme based on CNN and LSTM for urban $PM_{2.5}$ concentration. IEEE Access, 7(c): 20050–20059 **(10 pages)**.
26. Raaschou-Nielsen, O.; Antonsen, S.; Agerbo, E.; Hvidtfeldt, U.A.; Geels, C.; Frohn, L.M.; Christensen, J.H.; Sigsgaard, T.; Brandt, J.; Pedersen, C.B., (2023). $PM_{2.5}$ air pollution components and mortality in Denmark. Environ. Int., 171: 107685 **(8 pages)**.
27. Santos, C.F.G.D.; Papa, J.P., (2022). Avoiding overfitting: A survey on regularization methods for convolutional neural networks. ACM Comput. Surv., 54 (10): 1–22 **(25 pages)**.
28. Santoso, M.; Lestiani, D.D.; Kurniawati, S.; Damastuti, E.; Kusmartini, I.; Atmodjo, D.P.D.; Sari, D.K.; Hopke, P.K.; Mukhtar, R.; Muhtarom, T.; Tjahyadi, A.; Parian, S.; Kholik, N.; Sutrisno, D.A.; Wahyudi, D.; Sitorus, T.D.; Djamilus, J.; Riadi, A.; Supriyanto, J.; Dahyar, N.; Sondakh, S.; Hogendrop, K.; Wahyuni, N.; Bejawan, G.I.; Suprayadi, L.S., (2020). Assessment of urban air quality in Indonesia. Aerosol Air Qual. Res., 20(10): 2142–2158 **(17 pages)**.
29. Sareen, K.; Panigrahi, B.K.; Shikhola, T.; Sharma, R., (2023). An imputation and decomposition algorithms based integrated approach with bidirectional LSTM neural network for wind speed prediction. Energy. 278: 127799 **(26 pages)**.
30. Shao, X.; Kim, C.S., (2022). Accurate multi-site daily-ahead multi-step $PM_{2.5}$ concentrations forecasting using space-shared CNN-LSTM. CMC-Comput. Mater. Continua., 70(3): 5143–5160 **(18 pages)**.
31. Sun, Q.; Zhu, Y.; Chen, X.; Xu, A.; Peng, X., (2021). A hybrid deep learning model with multi-source data for $PM_{2.5}$ concentration forecast. Air Qual. Atmos. Health. 14(4): 503–513 **(11 pages)**.
32. Tabrizi, S.E.; Xiao, K.; Van G.J.; Saad, M.; Farghaly, H.; Yang, S.X.; Gharabaghi, B., (2021). Hourly road pavement surface temperature forecasting using deep learning models. J. Hydrol., 603: 126877 **(10 pages)**.
33. Utku, A., Can, U., Kamal, M., Das, N., Cifuentes-Faura, J., Barut, A., (2023). A long short-term memory-based hybrid model optimized using a genetic algorithm for particulate matter 2.5 prediction. Atmos. Pollut. Res., 14(8): 101836 **(13 pages)**.
34. Varshney, M.; Singh, P., (2021). Optimizing nonlinear activation function for convolutional neural networks. Signal, Image Video Process. 15(6): 1323–1330 **(8 pages)**.
35. Vrskova, R.; Hudec, R.; Kamencay, P.; Sykora, P., (2022). Human activity classification using the 3DCNN architecture. Appli. Sci., 12(2): 1–17 **(17 pages)**.
36. Xayasouk, T.; Lee, H.M.; Lee, G., (2020). Air pollution prediction using long short-term memory (LSTM) and deep autoencoder (DAE) models.

Sustainability, 12: 2570 **(17 pages)**.
37. Xiao, M.; Wu, Y.; Zuo, G.; Fan, S.; Yu, H.; Shaikh, Z.A.; Wen, Z., (2021). Addressing overfitting problem in deep learning-based solutions for next generation data-driven networks. Wireless Commun. Mobile Comput., 2021 **(10 pages)**.
38. Yang, J.; Yan, R.; Nong, M.; Liao, J.; Li, F.; Sun, W., (2021). $PM_{2.5}$ concentrations forecasting in Beijing through deep learning with different inputs, model structures and forecast time. Atmos. Pollut. Res., 12(9): 101168 **(13 pages)**.
39. Zhang, H.; Wang, Y.; Hu, J.; Ying, Q.; Hu, X.M., (2015). Relationships between meteorological parameters and criteria air pollutants in three megacities in China. Environ.Res., 140: 242–254 **(13 pages)**.
40. Zhang, M.; Shi, L.; Ma, X.; Zhao, Y.; Gao, L., (2021). Study on comprehensive assessment of environmental impact of air pollution. Sustainability. 13(2): 476 **(18 pages)**.
41. Zou, Y.; Wang, J.; Lei, P.; Li, Y. (2023). A novel multi-step ahead forecasting model for flood based on time residual LSTM. J. Hydrol., 620: 129521 **(15 pages)**.

AUTHOR (S) BIOSKETCHES

Istiana, T., Ph.D. Candidate, Department of Physics, Universitas Indonesia, Depok, Indonesia. Indonesia's Meteorological, Climatological, and Geophysical Agency, Central Jakarta, Jakarta, Indonesia.
- Email: *tri.istiana@sci.ui.ac.id*
- ORCID: 0000-0001-5535-1041
- Web of Science ResearcherID: NA
- Scopus Author ID: 58038019500
- Homepage: https://www.researchgate.net/profile/Tri-Istiana

Kurniawan, B., Ph.D., Associate Professor, Department of Physics, Universitas Indonesia, Depok, Indonesia.
- Email: *budhy.kurniawan@sci.ui.ac.id*
- ORCID: 0000-0002-9203-7438
- Web of Science ResearcherID: NA
- Scopus Author ID: 6602596727
- Homepage: https://physics.ui.ac.id/budhy-kurniawan/

Soekirno, S., Ph.D., Associate Professor, Department of Physics, Universitas Indonesia, Depok, Indonesia.
- Email: *santoso.soekirno@sci.ui.ac.id*
- ORCID: 0009-0000-3750-3371
- Web of Science ResearcherID: NA
- Scopus Author ID: 57202291516
- Homepage: https://physics.ui.ac.id/santoso-soekirno/

Wihono, A., B.Sc., Department of Physics, Universitas Indonesia, Depok, Indonesia.
- Email: *alvin.wihono@ui.ac.id*
- ORCID: 0000-0002-9044-1891
- Web of Science ResearcherID: NA
- Scopus Author ID: NA
- Homepage: https://www.researchgate.net/profile/Alvin-Wihono

Nuryanto, D.E., Ph.D., Indonesia's Meteorological, Climatological, and Geophysical Agency, Central Jakarta, Jakarta, Indonesia.
- Email: *danang.eko@bmkg.go.id*
- ORCID: 0000-0002-9637-5063
- Web of Science ResearcherID: NA
- Scopus Author ID: 56237657100
- Homepage: https://www.researchgate.net/profile/Danang-Nuryanto

Pertala, B.A., B.Sc., Indonesia's Meteorological, Climatological, and Geophysical Agency, Central Jakarta, Jakarta, Indonesia.
- Email: *boma.anjang@bmkg.go.id*
- ORCID: 0000-0002-1366-9067
- Web of Science ResearcherID: NA
- Scopus Author ID: 56237657100
- Homepage: https://www.linkedin.com/posts/boma-anjang-2b823918b_professional-google-workspace-administrator-activity-7184865878067326977-Auc0/

Sopaheluwakan, A., Ph.D., Deputy Head for Climatology, Indonesia's Meteorological, Climatological, and Geophysical Agency, Central Jakarta, Jakarta, Indonesia. World Meteorological Organization (WMO), Geneva, Switzerland.
- Email: *ardhasena@bmkg.go.id*
- ORCID: 0000-0002-4532-854X
- Web of Science ResearcherID: NA
- Scopus Author ID: 6506700584
- Homepage: https://www.researchgate.net/profile/Ardhasena-Sopaheluwakan

HOW TO CITE THIS ARTICLE

Istiana, T.; Kurniawan, B.; Soekirno, S.; Wihono, A.; Nuryanto, D.E.; Pertala, B.A.; Sopaheluwakan, B., (2024). Fine particulate matter concentrations forecasting using long short-term memory network and meteorological inputs. Global J. Environ. Sci. Manage., 10(4): 1759-1774.

DOI: 10.22034/gjesm.2024.04.16

URL: https://www.gjesm.net/article_713740.html